View metadata, citation and similar papers at core.ac.uk
brought to you by CORE
provided by Ulster University's Research Portal

Three-dimensional FE-EFGM adaptive coupling and its applications in the nonlinear adaptive analysis

Z. Ullah[a,*], C. E. Augarde[a], W. M. Coombs[a]

[a]*School of Engineering and Computing Sciences, Durham University, Durham DH1 3LE, UK.*

Abstract

Three-dimensional problems with both material and geometrical nonlinearities are of practical importance in many engineering applications, e.g. geomechanics, metal forming and biomechanics. Traditionally, these problems are simulated using an adaptive finite element method (FEM). However, the FEM faces many challenges in modeling these problems, such as mesh distortion and selection of a robust refinement algorithm. Adaptive meshless methods are a more recent technique for modeling these problems and can overcome the inherent mesh based drawbacks of the FEM but are computationally expensive. To take advantage of the good features of both methods, in the method proposed in this paper, initially the whole of the problem domain is modeled using the FEM. During an analysis those elements which violate a predefined error measure are automatically converted to a meshless zone. This zone can be further refined by adding nodes, overcoming computationally expensive FE remeshing. Therefore an appropriate coupling between the FE and the meshless zone is vital for the proposed formulation.

One of the most widely used meshless methods, the element-free Galerkin method (EFGM), is used in this research. Maximum entropy shape functions are used instead of the conventional moving least squares based formulations‘. These shape functions posses a weak Kronecker delta property at the boundaries of the problem domain, which allows the essential boundary conditions to be imposed directly and also helps to avoid the use of a transition region in the coupling between the FE and the EFG regions. Total Lagrangian formulation is preferred over the update Lagrangian formulation for modeling finite deformation due to its computational efficiency. The well-established error estimation procedure of Zienkiewicz-Zhu is used in the FE region to determine the elements requiring conversion to the EFGM. The Chung and Belytschko error estimator is used in the EFG region for further adaptive refinement. Numerical examples are presented to demonstrate the performance of the current approach in three dimensional nonlinear problems.

Keywords: FE-EFGM adaptive coupling; error estimation; finite deformation; elasto-plasticity; total Lagrangian

1. Introduction

To overcome the inherent mesh based difficulties in the FEM for modeling problems with both material and geometrical nonlinearities, various meshless methods have been proposed. In these methods only nodes are used for the problem discretization, which is an ideal way to model problems with large deformations and moving boundaries, without computationally expensive FE remeshing. Another advantage of these methods is in adaptive analysis, which is very straightforward as compared to the adaptive FEM, as nodes can be added and deleted without remeshing. On the other hand, meshless methods are unsuitable for the three-dimensional complicated real-life problems due to their high computational cost. Coupled FEM-meshless methods have been proposed in the literature to take advantage of the positive features of both methods. In these coupled methods, the meshless zone is used only in a region of the problem domain which is difficult to model with the FEM. The FEM can be used in the remaining part of the problem domain. Coupling between the FEM and meshless methods is not straightforward because meshless methods' shape functions generally do not posses the Kronecker delta property. There are a few methods available in the literature to couple the FEM and meshless methods but are limited to two-dimensional linear-elastic problems due to their computational complication. On the other hand, adaptive techniques have been used to increase the computational efficiency of meshless methods. However, existing approaches are also limited to linear-elastic and two-dimensional nonlinear problems.

In this research, a new hybrid FE-meshless procedure is proposed to simulate nonlinear problems with both material and geometrical nonlinearities based on a total Lagrangian formulation, where initially the whole of the problem is modeled with the FEM. During the simulation those finite elements which violate a predefined error measure are converted automatically to a meshless zone, which is then refined by adding nodes without computationally expensive FE remeshing. Limited literature is available on adaptive FE-meshless coupling, references [1, 2] deals only with two-dimensional

*Corresponding author
Email address: zahur.ullah@dur.ac.uk (Z. Ullah)

problems without proper error estimation and with no further adaptivity in the meshless zone. One of the of the most prominent meshless methods, the EFGM [3] is used in this research. In the conventional EFGM, moving least squares (MLS) shape functions are used for the approximation of the field variables; background cells are used for numerical integration and Lagrange multipliers used to enforce the essential boundary conditions in an approximate sense because the MLS shape functions do not possess the Kronecker delta property. The recently developed local maximum entropy (max-ent) shape functions [4] are used in the EFGM instead of the MLS shape functions. These shape functions possess a weak Kronecker delta property at the boundaries, which allows the imposition of essential boundary conditions directly as in the FEM. A new way to couple the EFGM with the FEM was proposed in [5] for linear and nonlinear problems using the max-ent shape functions in the EFG zone. As compared to the MLS shape functions, max-ent shape functions provide a natural way to couple the EFG and the FE zones due to the weak Kronecker delta property. This formulation removes the need for interface elements between the FE and the EFG zones, unlike the approach adopted by most researchers. This coupling procedure in [5] is extended here to adaptive coupling of the FE and the EFG zones. The nonlinear incremental form of Zienkiewicz and Zhu (or Z^2) error estimation based on the superconvergent patch recovery method [6, 7] is used to estimate error in the FE region. An error estimator similar in form to that developed by Chung and Belytschko (CB) [8, 9] is used to estimate error in the EFG zone.

2. Theoretical background

The formulations proposed in this work are based on the use of max-ent shape functions in the EFGM, the detail of which can be found in [9], in which updated Lagrangian formulation was used to model the finite deformation. In the updated Lagrangian approach, the variables are referred back to the updated geometry, which is updated at the end of each Newton-Raphson iteration, which includes update of nodal coordinates, Gauss points and calculation of new domains of influence and shape functions and the corresponding derivatives. Due to all of these involved computations updated Lagrangian formulation is computationally expensive for meshlesss methods. Total Lagrangian formulation is used in this paper, in which there is no need to update the geometry as the variables are referred back to the original configuration. Shape functions and the corresponding derivatives are calculated and stored only once for each new discretization and are used in all the Newton-Raphson iterations associated with it. For modeling the elasto-plasticity, the Prandtl-Reuss constitutive model is used, which comprises the von Mises yield function with perfect plasticity and associated flow. Effective plastic strain is used as one of the measures to evaluate the performance of the proposed model in the numerical examples and is given as

$$\overline{\boldsymbol{\varepsilon}^p} = \sqrt{\frac{2}{3}\left(\boldsymbol{\varepsilon}^p\right)^T\left(\boldsymbol{\varepsilon}^p\right)}, \tag{1}$$

where $\boldsymbol{\varepsilon}^p$ is plastic strain vector. Furthermore, consistent or algorithmic tangent is used to construct the global stiffness matrix, which leads to asymptotic quadratic convergence of the global Newton-Raphson algorithm.

Cubic spline weight functions are used to calculate the max-ent and MLS shape functions. The Voronoi diagram method is used to search for the set of surrounding nodes to calculate the nodal influence domains. Voro++ [10], which is an open source C++ software library for the generation of three-dimensional Voronoi diagrams for a set of particle in space is used in this research. Instead of brute force or exhaustive search algorithm, kd-tree (k-dimensional tree) with the background mesh algorithm [11] is used to search nodes in the support of Gauss points, i.e. to take advantage of the computational efficiency of background mesh and kd-tree algorithm simultaneously. Kd-tree is the generalization of the binary search algorithm to k dimensions and is commonly used in the computer sciences to organize data in k-dimensional space. The KDTREE2 [12] is used in this research, which is an open-source implementation of the kd-tree algorithm available as a FORTRAN-95 module.

For nonlinear problems, estimation of discretization error coupled with refinement strategy and data transfer between the evolving discretizations are main components of an adaptive procedure. For the recovery type, error estimation in these problems, the proposed in [7] is used, i.e. to calculate the incremental error in each solution step. For the solution step n, equations for the incremental error in energy norm and the corresponding energy norm for either an individual FE element or EFG background cell Ω_e are

$$\left\|e_e^p\right\| = \left[\int_{\Omega_e}\left|\left(\boldsymbol{\tau}_n^p\left(\mathbf{x}\right)-\boldsymbol{\tau}_n^h\left(\mathbf{x}\right)\right)^T\left(\Delta\boldsymbol{\varepsilon}_n^p\left(\mathbf{x}\right)-\Delta\boldsymbol{\varepsilon}_n^h\left(\mathbf{x}\right)\right)\right| d\Omega\right]^{\frac{1}{2}}, \qquad \left\|U_e\right\| = \left[\int_{\Omega_e}\left|\left(\boldsymbol{\tau}_n^p\left(\mathbf{x}\right)\right)^T\left(\Delta\boldsymbol{\varepsilon}_n^p\left(\mathbf{x}\right)\right)\right| d\Omega\right]^{\frac{1}{2}}, \tag{2}$$

where the subscript e shows an individual FE element or EFG background cell, $\boldsymbol{\tau}_n^p\left(\mathbf{x}\right)$ and $\boldsymbol{\tau}_n^h\left(\mathbf{x}\right)$ are the projected and approximate Kirchhoff stresses respectively at point $\mathbf{x}$ for solution step n, while $\Delta\boldsymbol{\varepsilon}_n^p\left(\mathbf{x}\right)$ and $\Delta\boldsymbol{\varepsilon}_n^h\left(\mathbf{x}\right)$ are the projected and approximate incremental logarithmic strains at a point $\mathbf{x}$ for the solution step n, that is

$$\Delta\boldsymbol{\varepsilon}_n^p\left(\mathbf{x}\right) = \boldsymbol{\varepsilon}_n^p\left(\mathbf{x}\right) - \boldsymbol{\varepsilon}_{n-1}^p\left(\mathbf{x}\right), \qquad \Delta\boldsymbol{\varepsilon}_n^h\left(\mathbf{x}\right) = \boldsymbol{\varepsilon}_n^h\left(\mathbf{x}\right) - \boldsymbol{\varepsilon}_{n-1}^h\left(\mathbf{x}\right). \tag{3}$$

The projected Kirchhoff stresses and the projected logarithmic strains' increments are found using the Z^2 and the CB procedure for the FEM and the EFGM respectively. Equations for the error in energy norm and the corresponding energy norm for the problem domain Ω are written as

$$\|e^p\|^2 = \sum_{i=1}^{n_{FE}} \left\|e^p_{FE}\right\|^2_i + \sum_{j=1}^{n_{EFG}} \left\|e^p_{EFG}\right\|^2_j, \qquad \|U\|^2 = \sum_{i=1}^{n_{FE}} \|U_{FE}\|^2_i + \sum_{j=1}^{n_{EFG}} \|U_{EFG}\|^2_j, \tag{4}$$

where n_{FE} and n_{EFG} are the total number of FE elements and EFG background cells respectively. Incremental global relative percentage error and permissible error in an individual FE element or EFG background cells are written as

$$\eta = \frac{\|e^p\|}{\|U\|} \times 100, \qquad \overline{\|e_e\|} = \frac{\overline{\eta}}{100}\left(\frac{\|U\|^2}{n}\right)^{\frac{1}{2}}, \tag{5}$$

where $n = n_{FE} + n_{EFG}$ and $\overline{\eta}$ is a permissible relative error for the whole problem domain. The adaptive procedure is triggered by the global relative error, i.e. $\eta > \overline{\eta}$ and the conversion of the FE elements to the EFG background cells or further refinement of the EFG background cells are based on $\frac{\|e^p_e\|}{\|e_e\|} > 1$. The corresponding two-dimensional step by step refinement strategy in the EFG zone is shown in Figure 1, which is straightforward to extend to three-dimensional problems. The refinement of the EFG zone, i.e. column A, B, C produces hanging nodes in the FE region, i.e. column D in Figure 1. To avoid the problem of dealing with the FE elements with hanging nodes; the strategy adapted in this work is to convert all those FE element to the corresponding EFG background cells.

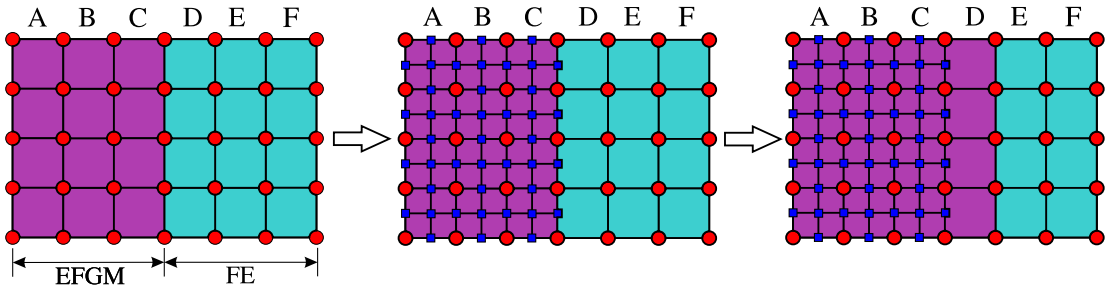

Figure 1: Refinement strategy

3. Numerical examples

Following two numerical examples are now given to demonstrate the correct implementation and performance of the full adaptive, hybrid FE-EFG modeling approach, whose components have been briefly described above. The scaling parameters for the domains of influence for analysis and projection used in the meshless zone are $d^a_{max} = 1.5$ and $d^p_{max} = 1.1$ respectively. The permissible relative error used are 25%.

3.1. 3D plate with a hole

The first numerical example is a three-dimensional plate with a central hole subjected to unidirectional tension. The full geometry for this problem is shown in Figure 2(a), out of which only one-eighth, shown in gray in the same figure, is modeled. The material properties used for this problem are $E = 1.0 \times 10^5$, $\nu = 0.3$ and $\sigma_y = 1.0 \times 10^3$, all in compatible units, where E, ν and σ_y are the modulus of elasticity, Poisson's ratio and yield strength. A total displacement of 0.15 unit is applied to the top face with 15 equal steps. The starting FE mesh with 325 nodes is shown in Figure 2(b), while the first conversions of the FE elements to the corresponding EFG background cells are shown in Figure 2(c). During this FE-EFG conversion, the degrees of freedoms remain the same. The Z^2 error estimator is used in the start of analysis because the discretization is based on only FE elements but after the first conversion a combine error estimator based on the Z^2, and the CB error estimator is used. Further conversion of the FE elements to the EFG zone and refinements of the EFG zone are shown in Figures 2(d) and 2(e) with 929, 4119 nodes respectively. The adaptive algorithm based on the combined Z^2 and CB error estimator automatically adds nodes in the thinning section of the plate as expected. The contours of the effective plastic strain are shown in Figure 3(a), in which a shear band of finite thickness next to the hole is clearly evident. Reaction/displacement plots are given in 3(b), the reaction being the integrated nodal loads along the displaced face, and the displacement is the prescribed displacement. The same problem is solved again with the different initial FE, and adaptive FE-EFG coupled discretizations shown in Figures 2(b), 2(c), 2(d) and 2(e) without adaptivity and the plots for reaction/displacement are also shown in Figure 3(b) for comparison. As compared to the coupled FE-EFG

response, the FE solution is very rigid without obvious geometric softening behaviour due to necking. The steps in the curve for the adaptive analysis are points where discretization changes. The reaction/displacement curve for the adaptive analysis and other different adaptive discretization without adaptivity converges to the solution of the final FE-EFG-3, which shows the effectiveness of the proposed adaptive coupled FE-EFG.

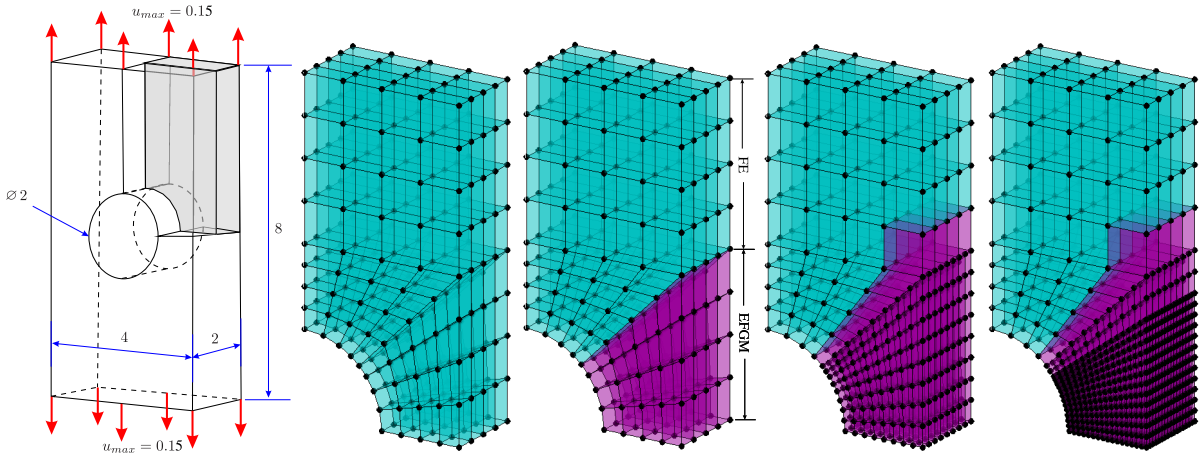

(a) Geometry) (b) FE (325 nodes) (c) FE-EFG-1 (325 nodes) (d) FE-EFG-2 (929 nodes) (e) FE-EFG-3 (4119 nodes)

Figure 2: Geometry and step by step discretizations for the 3D plate with a hole problem

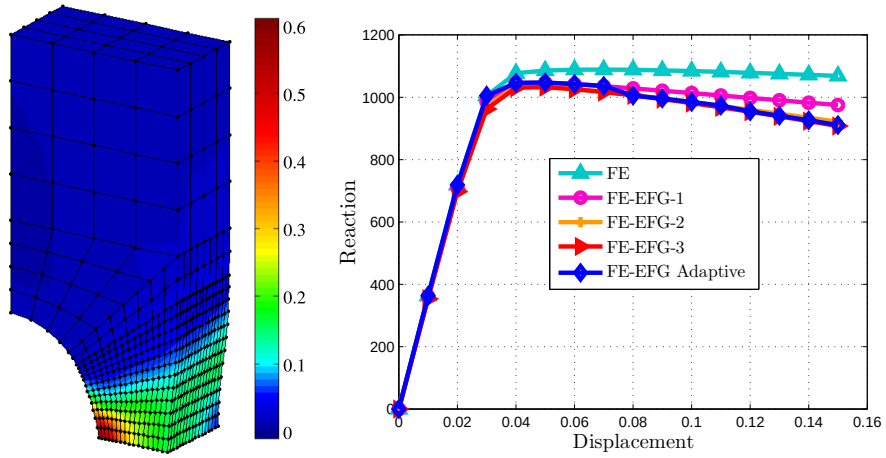

(a) Effective plastic strain (b) Reaction vs displacement

Figure 3: Effective plastic strain contours and Reaction vs displacement for the 3D plate with a hole problem

3.2. 3D footing loaded on a vertical cut

The second numerical example is a three-dimensional footing loaded next to unsupported faces of the soil as shown in Figure 4(a) with loading and dimensions. In this case, only soil section of the problem is modeled with a total vertical displacement of 0.1 unit applied to the nodes under the footing in 15 equal steps. The material properties used for this problem are $E = 2.0 \times 10^4$, $\nu = 0.3$ and $\sigma_y = 30$, all in compatible units. The starting FE mesh with 729 nodes is shown in Figure 4(b), and the step by step conversion of the FE elements to EFG zone and further refinement of the EFG zone are shown in Figures 4(c), 4(d) and 4(e) with 729, 1215, 2950 nodes respectively in the consecutive discretizations. For this problem, the adaptive algorithm based on the combined Z^2 and CB error estimator automatically adds nodes in the region where failure is expected in the soil and need more nodes for accurate modeling of slip lines. Contours of the effective plastic strain are shown in Figure 5(a) with a very clear shear band of finite thickness below the footing. A comparison between the reaction/displacement curves for the adaptive and different initial discretizations, shown in Figures 4(b), 4(c), 4(d) and 4(e) without adaptivity are also given in Figure 5(b). The curve for adaptive analysis and for different initial adaptive discretizations converges to a clear limiting load, which shows the effectiveness of the proposed adaptive

coupling. Furthermore, the curve for adaptive analysis initially follows the FE curve but after adaptivity it approaches the corresponding curves with the same discretizations.

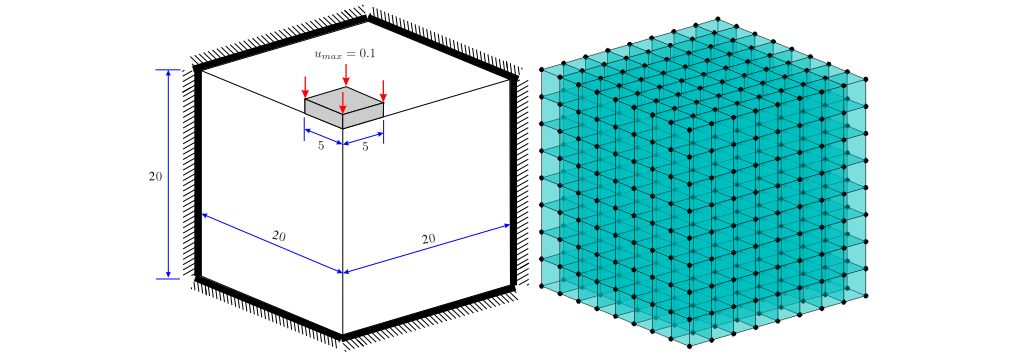

(a) Geometry) (b) FE (729 nodes)

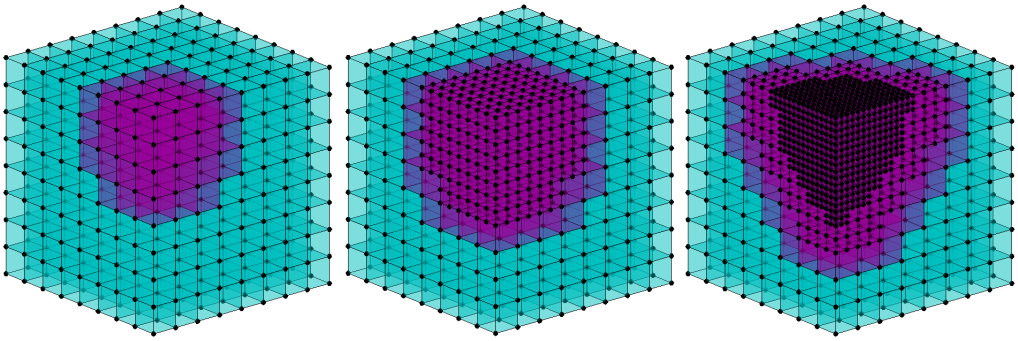

(c) FE-EFGM-1 (729 nodes) (d) FE-EFGM-2 (1215 nodes) (e) FE-EFGM-3 (2950 nodes)

Figure 4: Geometry and step by step discretizations for the 3D vertical cut problem

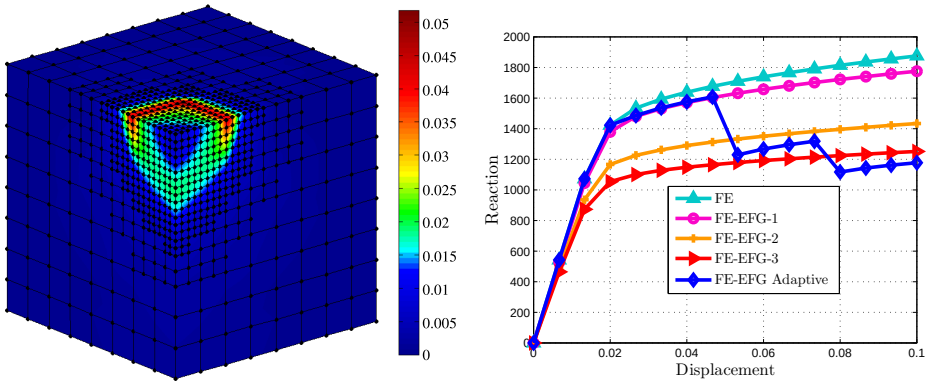

(a) Effective plastic strain (b) Reaction vs displacement

Figure 5: Effective plastic strain contours and Reaction vs displacement for the 3D vertical cut problem

4. Conclusions

In this paper, a new hybrid adaptively coupled FE-EFG numerical model is described for use in three-dimensional nonlinear solid mechanics based on total Lagrangian formulations. The model can accommodate both geometrical and material nonlinearity and includes automatic conversion from the FE to the EFG zone and further refinement in the EFG zone. The max-ent shape functions are used to approximate the field variables, which facilitates in both the imposition of the essential boundary conditions and in the coupling between the FE and the EFG zones. Error estimation based on the Z^2 and CB error estimator are used in the FE and the EFG zones respectively. A combined incremental error is calculated for each solution step and is used as the criterion to identify the FE elements for automatic conversion into EFG

background cells or their further refinement. The adaptive refinement in the EFG zone can take place very simply both due to the meshless approach and the chosen structured grids of nodes. MLS shape functions are used to transfer the path dependent variables from the consecutive discretization. Two challenging examples have been presented to demonstrate the capabilities of the new modeling procedure as a whole.

Acknowledgements

The first author is supported by an ORSAS from Durham University.

References

[1] H. Karutz, R. Chudoba, W. Krätzig, Automatic adaptive generation of a coupled finite element/element-free Galerkin discretization, Finite Elements in Analysis and Design 38 (11) (2002) 1075 – 1091.

[2] L. Liu, X. Dong, C. Li, Adaptive finite element-element-free Galerkin coupling method for bulk metal forming processes, Journal of Zhejiang University - Science A 10 (2009) 353–360.

[3] T. Belytschko, Y. Y. Lu, L. Gu, Element-free Galerkin methods, International Journal for Numerical Methods in Engineering 37 (1994) 229–256.

[4] N. Sukumar, R. W. Wright, Overview and construction of meshfree basis functions: from moving least squares to entropy approximants, International Journal for Numerical Methods in Engineering 70 (2007) 181–205.

[5] Z. Ullah, C. E. Augarde, R. S. Crouch, W. M. Coombs, FE-EFGM coupling using maximum entropy shape functions and its application to small and finite deformation, in: O. Laghrouche, A. EL Kacimi, P. Woodward, G. Medero (Eds.), 19th UK Conference on Computational Mechanics (ACME-UK), Heriot-Watt University, 2011, pp. 277–280.

[6] O. C. Zienkiewicz, J. Z. Zhu, The superconvergent patch recovery and a posteriori error estimates. Part 2: Error estimates and adaptivity, International Journal for Numerical Methods in Engineering 33 (7) (1992) 1365–1382.

[7] B. Boroomand, O. Zienkiewicz, Recovery procedures in error estimation and adaptivity. Part II: Adaptivity in non-linear problems of elasto-plasticity behaviour, Computer Methods in Applied Mechanics and Engineering 176 (1-4) (1999) 127 – 146.

[8] H.-J. Chung, T. Belytschko, An error estimate in the EFG method, Computational Mechanics 21 (1998) 91–100.

[9] Z. Ullah, C. Augarde, Finite deformation elasto-plastic modelling using an adaptive meshless method, Computers & Structures, in press (0). doi:http://dx.doi.org/10.1016/j.compstruc.2012.04.001.

[10] C. H. Rycroft, G. S. Grest, J. W. Landry, M. Z. Bazant, Analysis of granular flow in a pebble-bed nuclear reactor, Physical Review E 74 (2) (2006) 021306.

[11] E. Barbieri, M. Meo, A fast object-oriented Matlab implementation of the Reproducing Kernel Particle Method, Computational Mechanics 49 (2012) 581–602.

[12] M. B. Kennel, KDTREE 2: Fortran 95 and C++ software to efficiently search for near neighbors in a multi-dimensional Euclidean space (2004). doi:arXiv:physics/0408067.